Neuromuscular electrical stimulation improves skeletal muscle regeneration through satellite cell fusion with myofibers in healthy elderly subjects

Di Filippo ES[1,2], Mancinelli R[1,2,3], Marrone M[1,2], Doria C[1,2,3], Verratti V[1,3], Toniolo L[2,4], Dantas JL[3], Fulle S[1,2,3]* and Pietrangelo T[1,2,3]

[1]Department of Neuroscience Imaging and Clinical Sciences, 'G. d'Annunzio' University of Chieti–Pescara, Chieti, Italy

[2]Interuniversity Institute of Myology, Italy

[3]Laboratory of Functional Evaluation, 'G. d'Annunzio' University of Chieti–Pescara, Chieti, Italy

[4]Department of Biomedical Sciences, University of Padova, Padova, Italy

Running head: NMES and muscle regeneration in the elderly

***Corresponding author: Stefania Fulle**

Department of Neuroscience Imaging and Clinical Sciences

'G. d'Annunzio' University of Chieti–Pescara

Via dei Vestini, 31

66100 Chieti, Italy

Tel: +39-0871-3554555

Email: s.fulle@unich.it

26 **ABSTRACT**

27

28 The aim was to determine whether neuromuscular electrical stimulation (NMES)
29 affects skeletal muscle regeneration through a reduction of oxidative status in
30 satellite cells of healthy elderly subjects. Satellite cells from the *Vastus lateralis*
31 skeletal muscle of 12 healthy elderly subjects before and after 8 weeks of NMES
32 were allowed to proliferate to provide myogenic populations of adult stem cells
33 (myogenic precursor cells; MPCs). These MPCs were then investigated in terms of
34 their proliferation, their basal cytoplasmic free Ca^{2+} concentrations, and their
35 expression of myogenic regulatory factors (*PAX3, PAX7, MYF5, MYOD, MYOG*) and
36 microRNAs (miR-1, miR-133a/b, miR-206). The oxidative status of these MPCs was
37 evaluated through superoxide anion production and superoxide dismutase and
38 glutathione peroxidase activities. On dissected single skeletal myofibers, the nuclei
39 were counted to determine the myonuclear density, the fiber phenotype, cross
40 sectional area and tension developed. The MPCs obtained after NMES showed
41 increased proliferation rates along with increased cytoplasmic free Ca^{2+}
42 concentrations and gene expression of *MYOD* and *MYOG* on MPCs. The muscle-
43 specific miR-1, miR133a/b, miR-206 were up-regulated. This NMES significantly
44 reduced superoxide anion production, along with a trend to reduction of superoxide
45 dismutase activity. The NMES-dependent stimulation of muscle regeneration
46 enhanced satellite cells fusion with mature skeletal fibers. NMES improved the
47 regenerative capacity of skeletal muscle in elderly subjects. Accordingly, the skeletal
48 muscle strength and mobility of NMES-stimulated elderly significantly improved.
49 NMES may thus be further considered for clinical or ageing populations.

50

New & Noteworthy

The NMES effect on skeletal muscle regeneration was assessed on healthy elderly for the first time. NMES improved the regenerative capacity of skeletal muscle through increased MPC proliferation and fusion with mature myofibers. The increased $[Ca^{2+}]_{cyt}$ along with *MYOD*, *MYOG* and miRNAs up-regulation could be related to reduced $O_2^{\bullet-}$ production, which, in turn, favors myogenic regeneration. Accordingly, the skeletal muscle strength of NMES-stimulated lower limbs of healthy elderly subjects improved along with their mobility.

Keywords: neuromuscular electrical stimulation; satellite cells; superoxide anion; oxidative status; miRNA; elderly; superoxide dismutase activity; peroxidase activity, FTSST, TUG, strength.

Abbreviations

$[Ca^{2+}]_{cyt}$, cytoplasmic free Ca^{2+} concentration; miRNA, micro ribonucleic acid; MPCs, myogenic precursor cells; NMES, neuromuscular electrical stimulation; $O_2^{\bullet-}$, superoxide anion, *MYOG*, myogenin gene; FTSST, Five Times Sit-to-Stand Test; TUG, Time to Up-and-Go test.

72 **INTRODUCTION**

73

74 Elderly people experience skeletal muscle frailty, loss of myofibers, and dynapenia
75 (loss of muscle strength), which in one word can be defined as sarcopenia. As a
76 consequence, they can experience limited mobility, and, ultimately, mortality.
77 Moreover, sarcopenia can be exacerbated by neurological deficit and/or heavy
78 physical impairment, which, in turn, provoke immobilization. This condition often
79 represents the point of no return in the life of the elderly, because once it is reached,
80 these elderly people cannot perform volitional training, such as endurance or strength
81 training, which has been shown to maintain and increase human skeletal muscle also
82 for the elderly (25, 26, 54, 57).

83 In this scenario, an effective passive protocol that can be used to induce local
84 skeletal muscle contraction, such as neuromuscular electrical stimulation (NMES),
85 might be particularly useful to counteract the detrimental decline that occurs in
86 sarcopenic muscle. Indeed, it is commonly accepted that NMES can offer
87 advantages over voluntary training for people who have limited ability or are
88 noncompliant for volitional exercise, due to its promotion of specific motor unit
89 recruitment (20).

90 Effective skeletal fiber contraction involves recruitment and activation of
91 satellite cells in the muscle (57). *In vivo*, these quiescent satellite cells of postnatal
92 skeletal muscle fibers can be activated to the myogenic precursor cells (MPCs) that
93 are responsible for muscle growth and repair. Although it is currently accepted that
94 this skeletal muscle regeneration can be stimulated by exercise that involves
95 voluntary skeletal muscle contraction, debate still remains as to whether this also

96 occurs for atypical skeletal muscle contraction, such as contraction induced by
97 NMES.

98 Administration of an electrical current in the microampere range has been
99 successfully used to rescue atrophied mouse muscle (39). Furthermore, different
100 intensities of electrical stimulation (e.g., 2-20 Hz, 0.5-20 mA; 0.3 Hz, 10 μA) can
101 stimulate the proliferation of satellite cells/MPCs and myotube activity and rescue the
102 loss of myonuclei in atrophic and damaged mouse skeletal muscle (18, 21, 52).
103 Recently, an NMES protocol was described that is particularly suited to counteract
104 disuse muscle atrophy in men (20). Considering the strict link between atrophy and
105 sarcopenia and the involvement of MPCs in both of these conditions, we investigated
106 the effects of NMES on myogenesis in elderly human subjects.

107 We have previously shown that the human regenerative potential of satellite
108 cells derived from skeletal muscle of elderly subjects can be lost through
109 spontaneous increase in the apoptotic commitment of these cells (17). Our previous
110 investigations have suggested that the increased free radical production and
111 oxidative stress that can become established in MPCs from elderly subjects can act
112 as signals for maladaptive phenomena (10, 45, 50). More specifically, accumulation
113 of the superoxide anion ($O_2•^-$) is involved in the establishment of oxidative stress in
114 these MPCs (10). This $O_2•^-$ is one of the most dangerous oxidant species, and it is
115 mainly produced by mitochondria that have undergone metabolic impairment (37,
116 51). Here, the key element becomes the amount of $O_2•^-$ production and the
117 enzymatic defense that can be adopted by the cells. Indeed, low intensity training
118 mainly induces a significant $O_2•^-$ reduction in MPCs from healthy young muscle (48).
119 However, in some subjects, this training can instead produce a slight $O_2•^-$ increase
120 (48). In contrast, in MPCs of elderly subjects, the $O_2•^-$ levels and the generic

121 cytosolic oxidation levels are at least one third more than those in MPCs of young
122 subjects (10). This oxidative stress can provoke extensive cellular damage,
123 apoptosis, and inflammation of skeletal fibers and the satellite cell pool (13, 14, 16).
124 In this scenario, it is important to find stimuli that can be used to reduce the oxidative
125 stress, in order to reduce the signals for inflammation and to promote muscle mass
126 conservation and increased satellite cell stimulation in the elderly.

127 Some early evidence has demonstrated that NMES can increase intracellular
128 defenses against reactive oxygen species in skeletal muscle of young subjects (20).
129 Moreover, NMES has been shown to promote hypertrophy of the human *Vastus*
130 *lateralis* skeletal muscle and to increase the maximal force of the quadriceps in
131 young subjects (36). On the basis of all of this information, we asked whether NMES
132 can influence the regeneration process and the oxidative stress of activated satellite
133 cells (i.e., MPCs) in skeletal muscle of healthy elderly subjects. In particular, we
134 investigated these MPCs *in-vitro*, in terms of their proliferation and differentiation into
135 myotubes and fusion with myofibers, their basal cytoplasmic free Ca^{2+} concentration
136 ($[Ca^{2+}]_{cyt}$), and their gene expression of myogenic regulatory factors (*PAX3*, *PAX7*,
137 *MYF5*, *MYOD*, *MYOG*) and microRNAs (miR-1, miR-133a/b, miR-206), prior to and
138 following NMES. The oxidative status of these MPCs through $O_2^{\bullet -}$ production and the
139 superoxide dismutase and glutathione peroxidase activities were also investigated.
140 Moreover, the measurement of maximal voluntary contraction on elderly lower limbs
141 permitted to relate the cellular and molecular adaptation of NMES-stimulated skeletal
142 muscle to the effectiveness of this protocol.

143

144 **MATERIALS AND METHODS**

145 ***Subjects***

146 Twelve healthy male elderly subjects (69.5 ±1.6, age) volunteered to participate in
147 this study. They used to have an active lifestyle, but were not engaged in any specific
148 exercise training protocols (≥6 months) before their enrolment in this study. One
149 week before and 2 days after the NMES sessions, these subjects had their height,
150 weight, body fat measured, and their body mass index was calculated. Their bilateral
151 isometric maximal voluntary contraction (MVC) of the lower limbs was measured
152 using a leg-extension device (Nessfit Srl, San Giovanni Teatino, Italy) that was
153 equipped with loading cell to measure the strength output (Globus, Codognè, Italy).
154 The subjects remained in a seated position on the leg-extension device with their
155 knees at 90° and they performed a MVC for 5s using both legs. The test was
156 performed three times and the recovery time between tests was 2 min. The highest
157 value recorded was used as the MVC (46).

158 ***Functional Assessment and tiny percutaneous needle biopsy***

159 ***Five Times Sit-to-Stand Test (FTSST):*** the FTSST was applied as described in a
160 previous study using a 43-cm high chair. After a signal from the evaluator, the
161 volunteers stood up and sat down 5 times as quickly as possible, maintaining their
162 arms crossed on their chest. Before the test, the evaluator provided instructions to
163 the volunteers for a standardized execution: 1) "You need to maintain your arms
164 crossed on your chest during the entire test"; 2) "You need to stand up and sit down
165 5 times as quickly as you can when I say 'Go'"; 3) "The test begins when I say "Go"
166 and stops when you completely touch the chair on the fifth repetition"; 4) "You need
167 to stand up fully and touch the chair in every repetition, but you should not touch your
168 back to chair backrest during the test" (58). Volunteers performed the FTSST three
169 times. The first set consisted of a submaximal performance for test familiarization.

170 The final two sets were performed to calculate the reliability and typical error of the
171 FTSST, the best performance being considered for the analyses.
172 ***Timed Up and Go test (TUG):*** The TUG was applied as described in a previous
173 study119. The volunteers were required to stand up, walk 3 m, turn, walk back, and
174 sit down. Time to complete this task was the performance variable, evaluating
175 mobility capacity. Two evaluators were positioned on opposite sides of the walking
176 course (one at between 0 - 1.5m and another at between 1.5 – 3.0m) to avoid any
177 serious consequences in the case of a fall. As in the FTSST, the volunteers
178 performed the TUG three times, for the familiarization and reliability purposes
179 One day after the functional test, the tiny percutaneous needle biopsies of the
180 *Vastus lateralis* muscles were performed. The biopsy of the VL muscle was
181 performed at a level about one-third of the distance from the upper margin of the
182 patella to the trochanter major. The choice of this position was motivated by the
183 anatomical consideration that the area lacks significant neurovascular structures. For
184 this reason the tiny percutaneous needle biopsy procedure was well tolerated. More
185 detailed information has been extensively described in Pietrangelo et al 2011 and
186 2013 (43, 47).
187 This study was approved by the Ethics Committee of the 'G. d'Annunzio'
188 University of Chieti–Pescara, Italy (protocol nos. 1233/06 and 1884 COET), and it
189 was conducted according to the Helsinki Declaration. All of the subjects who
190 participated signed their informed consent.
191
192 ***Neuromuscular electrical stimulation sessions***
193 The NMES protocol consisted of a training program that lasted 18 min. The 12
194 subjects performed 40 passive isometric bilateral contractions that were stimulated

195 by a NMES device (Genesy 1200 Pro; Globus Srl, Codognè, Italy). This was applied
196 for three sessions per week over an 8-week period. During the NMES session, the
197 subjects were seated on a leg extension machine (NSFT 07036; Nessfit Srl, San
198 Giovanni Teatino, Italy) with the knee joint fixed at 90° knee extension, to provide the
199 isometric condition during the stimulation. Two active electrodes (contact area, 25
200 cm^2) were positioned over the motor points of the quadriceps muscles, as close as
201 possible to the motor point of the *Vastus lateralis* and *Vastus medialis* muscles. A
202 dispersive electrode (contact area, 50 cm^2) was placed 5 cm to 7 cm below the
203 inguinal crease, to close the stimulation loop. Rectangular-wave pulsed currents (75
204 Hz every 400 μs) were delivered with a rise time of 1.5 s, a steady tetanic stimulation
205 time of 4 s, and a fall time of 0.75 s (total duration of contraction, 6.25 s). A rest
206 interval of 20 s was provided between stimulations. The intensity was monitored and
207 recorded for each 5-min period. The intensity of the NMES was gradually increased
208 to an individual maximally tolerable intensity, which corresponded to the pain
209 threshold of each subject. The subjects were motivated to adjust their intensity during
210 the training session to maintain the maximum tolerable intensity throughout the
211 session, reaching at the end of the training period an intensity of 40 ±16 mA.
212
213
214 ***Satellite cell population and myogenicity***
215 A part of the tiny percutaneous muscle biopsies (about 10 mg) was treated to obtain
216 the muscle cells (43). The progeny of *in-vitro* satellite cells, MPCs, were initially
217 expanded in growth medium, and differentiated into myotubes as previously
218 described (15, 45, 48). These MPCs from the *Vastus lateralis* of the 12 healthy
219 elderly subjects were obtained before the NMES sessions were started, and after

220 they were completed, with these samples defined as pre-NMES and post-NMES,
221 respectively.

222 Briefly, the percentages of myogenicity were obtained by counting the MPCs
223 that were positive for an antibody against desmin (15), with respect to all of the cells
224 present in the field of view. We counted 6341 and 6369 cells on pre- and post-NMES
225 samples, respectively. At a confluence of 70% to 80%, the cells were split and the
226 population doubling level (PDL) was calculated. This is given by the ratio between
227 the number of cells that were detached (Nd) with respect to the number of cells that
228 were initially seeded (Ns; i.e., Nd/Ns), and log Nd/Ns was calculated and divided by
229 ln 2. The MPCs controls derived from TPNB samples of subjects without NMES were
230 analyzed as previously described.

231 The differentiation of these MPCs into myotubes was measured in terms of
232 the multinucleated cells that were positive to the primary antibody against myosin
233 heavy chain after 7 days of differentiation. This is reported as the Fusion Index, as a
234 percentage defined by counting the numbers of nuclei present in the myotubes, with
235 respect to the total number of nuclei in the observed field (i.e., nuclei in myotubes/
236 total nuclei ×100%). Myotubes were defined as those that were positive to the
237 primary antibody against myosin heavy chain and that had at least two nuclei (48).
238 We counted 2717 and 2731 cells on pre- and post-NMES samples, respectively.
239 Moreover, in the samples that were differentiated for 7 days, the numbers of
240 mononucleated desmin$^+$ cells were counted, which represents the number of
241 myogenic cells that were not able to fuse into multinucleated myotubes. We counted
242 2150 and 2139 cells on pre- and post-NMES samples, respectively.

243

244 ***Myonuclear density of single myofibers***

245 Another part of the tiny percutaneous muscle biopsies (about 5 mg) from four of
246 these subjects was manually dissected to obtain single skeletal myofibers (47). The
247 myonuclei along these single myofibers were counted, to determine the nuclear
248 domain. Briefly, to localize the nuclei, single myofibers were stained with DAPI (25
249 µg/mL; Sigma) for 10 min. To precisely measure the volume, the fibers have been
250 stained with a monoclonal mouse antibody anti-α-actinin (clone EA-53 Sigma). The
251 myonuclear density was determined as the number of nuclei in a constant myofiber
252 volume (10^6 μm^3). A confocal microscope (Vico; Nikon) was used to acquire the
253 fluorescent images (32, 40).
254
255 ***Mechanical features and phenotype of single fibers***
256 Muscle biopsy fragments for single fiber were stored at -20˚C and analyzed within 2
257 weeks of sampling. The biopsies were stored in skinning solution with 50% (v/v)
258 glycerol until day of the experiment. This solution contains high-potassium and high-
259 EGTA concentration that depolarizes membranes, removes calcium, and induces a
260 rigor to ensuring optimal conditions for fiber preservation. Before the analysis, the
261 skinning-glycerol mixture was replaced with ice-cold skinning solution containing
262 ATP, to induce fiber relaxation. From each biopsy single fibers were manually
263 dissected using a stereo-microscope (x10-60 magnification). Following dissection,
264 fibers were bathed for 10 min in skinning solution containing 1% (v/v) Triton X-100 to
265 completely have the membranes in solution. Fiber segments of 1-2 mm in length
266 were cut, and light aluminum clips were applied at both ends. Then they were
267 transferred to the experimental apparatus, and cross-sectional area (CSA) and
268 tension development during maximal calcium-activated isometric contractions at
269 12˚C were measured according to a previously described procedure (56, 41). At the

270 end of the experiment, each fiber was collected and put in Laemmli solution for
271 electrophoretic analysis (see below). All solutions employed for single fiber
272 experiments were prepared as described previously (7).
273

274 ***Electrophoretic separation and quantification of myosin heavy chain isoforms***

275 The fibers were characterized for their myosin heavy chain (MyHC) isoform. Muscle
276 biopsy fragments were solubilized in an appropriate volume of Laemmli solution (Tris
277 62.5 mM, Glycerol 10% [v/v], SDS 2.3% [w/v], ß-mercaptoethanol 5% [v/v], with E-64
278 0.1% [w/v] and leupeptin 0.1% [w/v] as anti-proteolytic factors; pH 6.8) and stored at -
279 80 °C until the analysis. Appropriate amounts (~10 µg of total protein/lane) of the
280 protein suspension were diluted in loading buffer (Laemmli solution with 0,01%
281 bromophenol blue) and boiled for 5 min at 80˚C before loading onto polyacrylamide
282 gels. Separation of MyHC isoforms was carried out on 8% (w/v) gels (18 cm x 16 cm
283 x 1 mm) at 70 V for 1.5 h and at 230 V for a further time according to the guidelines
284 of Talmadge and Roy (1993). The gels were stained with Coomassie-blue dye. After
285 staining, three separate bands were detected in the 200-kDa region, corresponding
286 to MyHC-1, -2A, and -2X, in order of migration from fastest to slowest. For each
287 biopsy sample fragment, at least two independent electrophoretic runs were
288 performed. Gel patterns were digitized with an HP Scanjet G4050 at a resolution of
289 1,200 dpi. The myosin isoforms distribution was achieved by densitometric analyses
290 of the bands after staining with Coomassie-blue. Each band was characterized by a
291 value of the Brightness-Area Product (BAP), after black/white inversion employing LI-
292 COR®Image Studio Lite (ver 5.0). From each line, BAP values for the bands
293 identified as MyHC isoforms were summed and the BAP value for each isoform was
294 expressed as a percentage of the total and the mean values of myosin isoforms

295 distribution for all subjects were obtained. The reproducibility of the procedure was
296 confirmed by calculating isoform ratios of selected samples from gels loaded with
297 different amounts of such samples.
298

299 ***Intracellular calcium concentrations***

300 The MPCs were loaded with Fura2-AM (final concentration, 5 μM) for 30 min,
301 washed by gentle solution removal and incubated for a further 30 min at 37 °C prior
302 to the $[Ca^{2+}]_{cyt}$ measurements, to allow the intracellular Fura2-AM de-esterification
303 (27). The experiments were performed and images were acquired using the
304 procedures and set-up described by Pietrangelo et al. (44). Thapsigargin (1 μM;
305 Sigma-Aldrich T9033), a known releaser of internal Ca^{2+} stores, was added in the
306 MPCs to induce the emptying of the intracellular Ca^{2+} stores. The thapsigargin-
307 dependent $[Ca^{2+}]_{cyt}$ transients was recorded for at least 2 min, and analysis of the
308 area under the 2-min transients was performed using the specific 'area under the
309 curve' function of GraphPad Prism Software, version 5 (GraphPad Software, La Jolla,
310 USA).
311

312 ***Reactive oxygen species***

313 The superoxide anion ($O_2\bullet^-$) levels were determined using the conventional assay
314 based on the dye nitroblue tetrazolium chloride (Cat. No. N6639; Sigma-Aldrich),
315 which is reduced to formazan by $O_2\bullet^-$, determined at 550 nm using a fluorometer
316 (SPECTRAmax Gemini XS; Molecular Devices Toronto, Canada (10, 48).

317 The cellular oxidant levels were determined using the dye 2,7-
318 dichlorofluorescein diacetate (DCF, Cat.No. D6883; Sigma). The fluorescence was
319 determined at 530 nm (excitation, 490 nm) using a fluorometer (SPECTRAmax

320 Gemini XS; Molecular Devices Toronto, Canada), with the data analyzed using the
321 SOFTmax Pro software (48).
322
323 ***Antioxidant enzyme activity***
324 The antioxidant enzyme activities of superoxide dismutase and glutathione
325 peroxidase (53, 55) were analyzed for the cytosolic fractions of undifferentiated
326 MPCs. The superoxide dismutase activity, where 2 $O_2{\bullet}^-$ (+ 2 H^+) is oxidized to form
327 O_2 and H_2O_2, was determined as previously described (48). The glutathione
328 peroxidase enzymatic activity was determined according to Shakirzyanova et al. (53),
329 and reported as specific activities.
330
331 ***Western blotting***
332 Western blotting (WB) analysis was performed on 40 μg lysates from pre- and post-
333 NMES MPCs, using SOD1 (71G8) mouse mAb (#4266, Cell Signalling Technology,
334 Danvers, MA, USA) at 1:1000, SOD2 (D9V9C) rabbit mAb (#13194, Cell Signalling
335 Technology) at 1:1000, β-Actin (8H10D10) mouse mAb (#3700, Cell Signalling
336 Technology) at 1:1000, as primary antibody. Secondary HRP-conjugated antibodies
337 (Cell Signalling Technology) at 1:5000. Bands were detected and pictured at Bio-Rad
338 GelDoc by LiteAblot PLUS enhanced chemiluminiscent substrate (EuroClone);
339 densitometry analyses were performed with ImageJ software (10).
340
341 ***Quantitative real-time PCR for myogenic transcriptional factors and miRNAs***
342 The RNA was extracted from the PMCs using Purelink RNA mini kits (Invitrogen, Life
343 Technologies), as described by Di Filippo et al. (10). Briefly, 500 ng extracted RNA
344 was reverse transcribed using Superscript III First-Strand Synthesis SuperMix kits

345 (Invitrogen, Life Technologies). Quantitative real-time PCR was performed on 1:5
346 diluted cDNA, using Platinum Sybr Green SuperMix-UDG (Invitrogen, Life
347 Technologies). The myogenic regulatory factors investigated were: *PAX3, PAX7,*
348 *MYF5, MYOD, and MYOG*. GAPDH was used as the housekeeping gene, and the
349 data are shown as ΔCt.

350 PureLink miRNA isolation kits were used for the miRNA extractions (Cat. No.
351 K1570-01; Invitrogen, Life Technologies, Molecular Devices, Sunnyvale, USA),
352 according to Di Filippo et al. (10). The relative quantification of the miRNA targets
353 was carried out using the ΔCt formula. The specific miRNA sequence probes used
354 have the following catalog numbers: hsa-miR-16-5p, #000391; hsa-miR-1, #002222;
355 hsa-miR-206, #000510; hsa-miR-133b, #002247; hsa-miR-133a, #002246. miR-16
356 was used as the housekeeping gene, and the data are shown as ΔCt. Three
357 independent experiments were performed, each carried out in triplicate.

358

359

360 ***Statistical analysis***

361 The statistical analysis was carried out using the GraphPad Prism Software, version
362 5 (GraphPad Software, La Jolla, USA). The data are reported as means ± standard
363 error (SE) or standard deviation (SD). Unpaired and paired t-tests were used to
364 reveal statistical differences between cellular populations and single myofiber
365 analysis, respectively, at pre- and post-NMES.

366 Mixed analysis of variance (mixed ANOVA) was used to analyze differences between
367 groups and over time (control vs NMES-stimulated elderly) in addition to Bonferroni
368 post hoc comparisons.

369 Significance was indicated as *p $\leq$0.05, **p $\leq$0.005, and ***p $\leq$0.0001.

370

371 **RESULTS**

372

373 ***Maximal voluntary contraction of elderly subjects***

374 The anthropometric characteristics of the 12 healthy elderly subjects who participated
375 in the NMES sessions did not vary significantly (Table 1). However, compared to the
376 pre-NMES maximal voluntary contractions, the post-NMES values showed a
377 significant increase as well as the FTSST and TUG (Table 1).

378

379 Table 1 to be inserted about here

380

381 ***Myogenic characteristics and analysis of MPC differentiation***

382 The myogenic characteristics of the MPCs are reported in Table 2. Here, from pre-
383 NMES to post-NMES, there were no significant differences in the MPC myogenicity
384 (i.e., number of desmin$^+$ cells), Fusion Index, and desmin$^+$ nonfused MPCs at 7 days
385 of differentiation, as for control samples (data not shown).

386

387

388 Table 2 to be inserted about here

389

390 ***Proliferation rate* in vitro**

391 The PDLs of the pre-NMES and post-NMES MPCs were calculated at each passage,
392 when the cells reached about 80% confluence. As can be seen in Figure 1, the pre-
393 NMES MPCs reached 10 PDL in 50 days to 120 days (panel a), while the post-
394 NMES MPCs of the same subjects reached the same PDL in 30 days to 35 days

395 (panel b), demonstrating an increased rate of MPC proliferation post-NMES, similar
396 for all subjects. The MPCs controls, without NMES stimulation, reached 10 PDL in
397 35-40 days, showing a similar proliferation trend of pre-NMES MPCs (data not
398 shown).
399
400
401 Figure 1 to be inserted about here
402
403 ***Myonuclear density on single mature myofibers***
404 The single mature myofibers showed significant increases from pre-NMES to post-
405 NMES for the myonuclei fused to the myofibers ($p \leq 0.05$; Figure 2).
406
407 Figure 2 to be inserted about here
408
409 ***MyHC fiber phenotype***
410 The fiber type composition of the *Vastus Lateralis* muscle was determined by
411 analyzing the proportion of slow (MyHC-1) and fast (MyHC-2A and -2X) myosin
412 heavy chain isoforms in pre- and post-NMES biopsy samples. The average
413 percentage of fibers that express the specific MyHC isoform are shown in Figure 3. In
414 our sample, slow MyHC-1 fibers were significantly increased in post-NMES
415 compared to pre-NMES ($p \leq 0.05$). The percentage of fast MyHC-2A fibers did not
416 significantly vary whereas that of MyHC-2X ones showed a decrease not statistically
417 significant.
418
419 Figure 3 to be inserted about here

420

421 ***Muscle fiber cross-sectional area and specific tension***

422 The results on single muscle fibers (n=80) are displayed in the Figure 4. The CSA
423 was significantly incremented at post-NMES *vs* pre-NMES (5,810±267 μm^2 *vs*
424 4,983±288 μm^2, $p \leq 0.05$). The average force (F_o) significantly increased of about
425 20%, from 1.06±0.06 mN to 1.25±0.05 in post-NMES ($p \leq 0.05$).
426 The value of specific tension (Po), the isometric strength per unit of fiber area
427 (F_o/CSA), was 126.0±6.7 mN mm^{-2} and 137.8±7.7 mN mm^{-2} in pre- and post-NMES,
428 respectively. Although P_o tended to increase, this increment was not statistically
429 significant.

430

431 Figure 4 to be inserted about here

432

433 ***Cytoplasmic free Ca^{2+} concentrations of undifferentiated MPCs***

434 The basal $[Ca^{2+}]_{cyt}$ were significantly increased in the undifferentiated MPCs from
435 pre-NMES to post-NMES ($p \leq 0.05$; Figure 5a). The analysis of the time courses of
436 the Ca^{2+} released from the intracellular stores by thapsigargin (Figure 5b)
437 demonstrated that in these undifferentiated MPCs, from pre-NMES to post-NMES,
438 there was less Ca^{2+} released. The analysis of the area under the curve for these
439 thapsigargin-dependent $[Ca^{2+}]_{cyt}$ changes from pre-NMES to post-NMES showed a
440 significant reduction ($p \leq 0.001$; Figure 5c).

441

442 Figure 5 to be inserted about here

443

444 ***Myogenic regulatory factor gene expression profiles***

445 For the undifferentiated MPCs, from pre-NMES to post-NMES, the myogenic
446 transcription factors *PAX3, PAX7, MYF5* did not change their expression levels, while
447 *MYOD* and *MYOG* were significantly up-regulated ($p \leq 0.05$ and $p \leq 0.0001$,
448 respectively; Figure 6).
449
450 <u>Figure 6 to be inserted about here</u>
451
452 ***Superoxide anion production and basal levels of oxidant species***
453 The undifferentiated MPCs from pre-NMES to post-NMES showed significant $O_2 \bullet^-$
454 decrease (by about 40%) (Figure 7a).
455 The DCF fluorescence did not vary significantly from pre-NMES to post-NMES
456 (data not shown).
457
458 ***Antioxidant enzyme activity***
459 The activity of the cytosolic fractions from pre-NMES to post-NMES for the
460 antioxidant enzyme superoxide dismutase showed a decrease trend (31.8 ±1.4 *vs.*
461 29.7 ±1 U superoxide dismutase ng^{-1}; Figure 7b). Instead, the glutathione peroxidase
462 enzymatic activity remained the same from pre-NMES to post-NMES (0.25 ±0.06 *vs*.
463 0.27 ±0.05, data not shown).
464
465 <u>Figure 7 to be inserted about here</u>
466
467 ***SOD1 and SOD2 protein expression***.

468 A representative SOD1 and SOD2 bands obtained by MPCs at pre- and post-NMES
469 was shown in Figure 8a. The amount of both SOD cytosolic type 1 and mitochondrial
470 type 2 were reported in Figure 8b and c, by Western blotting analysis.
471
472 Figure 8 to be inserted about here
473
474 **Epigenetic miRNA profile**
475 The analysis of the miRNA expression from pre-NMES to post-NMES showed
476 significant up-regulation of miR-1, miR-133a, miR-133b and miR-206 ($p \leq 0.0001$;
477 Figure 9).
478
479 Figure 9 to be inserted about here
480
481 **DISCUSSION**
482 The lowered regenerative potential of satellite cells that occurs during human ageing
483 is known to be linked to the accumulation of oxidant species like $O_2{\bullet}^-$, together with
484 inadequate scavenger activity. These effects provoke cellular damage and impair the
485 ability of satellite cells to efficiently divide to the MPCs that can differentiate to sustain
486 muscle mass and function (5, 10, 12, 15, 30, 45). The hypothesis for the present
487 study was that NMES positively stimulates skeletal muscle regeneration of healthy
488 elderly subjects through a reduction in the MPC oxidation levels.
489 The data here for the MPC populations obtained after the NMES (i.e., post-
490 NMES) suggest that this procedure can promote increased proliferation rate along
491 with increased fusion of these adult stem cells with the existing myofibers.

492 We investigated some of the potential molecular aspects as key elements of
493 this regeneration process, in terms of $[Ca^{2+}]_{cyt}$ homeostasis, muscle regulating
494 transcription factors and miRNA expression, and oxidative species management.

495 In these undifferentiated MPCs, these data showed a post-NMES reduction in
496 the $[Ca^{2+}]_{cyt}$ of the (thapsigargin-releasable) intracellular Ca^{2+} stores in favor of an
497 increase in the basal $[Ca^{2+}]_{cyt}$. This is in line with the increased ability of these post-
498 NMES MPCs to fuse with existing myofibers (6, 27, 29). The release of the free Ca^{2+}
499 from intracellular stores occurs during the early steps of myoblast differentiation (3),
500 when a proliferative boost is required (33, 42). On this basis, our data confirm the
501 increased proliferation rate in the post-NMES MPCs. The NMES-dependent $[Ca^{2+}]_{cyt}$
502 increase might influence the fusion process via two key Ca^{2+}-dependent enzymes,
503 the transcription factor nuclear factor of activated T cells (NFAT) and the protein
504 kinase CamKII, which stimulate myogenin (2). Indeed an increase in $[Ca^{2+}]_{cyt}$ is
505 required for activation of myogenic transcription factors, such as myogenin (1).
506 Accordingly, myogenin gene expression was significantly up-regulated here. It is also
507 worth mentioning that this gene was not linked to myotube formation, because the
508 Fusion Index was similar here between the pre-NMES and post-NMES MPCs,
509 although we believe that it is instrumental for MPC fusion with existing myofibers.
510 Indeed, the post-NMES MPCs showed increased proliferation rate along with no
511 MYF5, PAX3 and *PAX7* variation but *MYOD* overexpression, with respect to pre-
512 NMES MPCs. It has been extensively demonstrated that this specific transcription
513 factor regulation occur when MPCs were committed to fusion escaping the self-
514 renewal (8).

515 Considering the importance of oxidative stress in human satellite cells, and its
516 role in impairment of regenerative processes in the elderly, we investigated the redox

517 balance of these pre-NMES and post-NMES MPCs. Surprisingly, the post-NMES
518 MPCs showed significant reduction (about 40%) in $O_2{\bullet}^-$ production even in the
519 presence of increased number of MyHC-1 fibers, the slow ones, those that rely
520 mostly on mitochondrial oxidative metabolism.

521 Superoxide dismutase and glutathione peroxidase are the most important
522 antioxidant enzymes for detoxification of $O_2{\bullet}^-$ and its derivative H_2O_2, respectively,
523 but these did not show different activities between the pre-NMES to post-NMES
524 MPCs. Moreover, the reduced trend of superoxide dismutase activity is in agreement
525 with both the decreased $O_2{\bullet}^-$ production and the mitochondrial SOD2 protein
526 reduction we found on post-NMES MPCs. Superoxide dismutase reduces $O_2{\bullet}^-$ to
527 H_2O_2, which is then a substrate for glutathione peroxidase. In the present study, the
528 glutathione peroxidase activity did not change. It might be that H_2O_2 that was also
529 produced through oxygen reduction by other metabolic sources did not decrease with
530 the $O_2{\bullet}^-$, and as a consequence, the glutathione peroxidase activity of the post-
531 NMES MPCs remained similar to that of the pre-NMES MPCs. In accordance, the
532 data on general cellular peroxidation performed using DCF fluorescence, revealed
533 that the cellular peroxidation end products measured directly on cells did not vary
534 between pre- and post-NMES. It may be that the period of 8 weeks of stimulation
535 was not sufficient to reduce the MPC general oxidative state in elderly, as expected
536 considering the $O_2{\bullet}^-$ reduction. Under another point of view, it is also interesting that
537 the general oxidation did not increase even in the presence of increased percentage
538 of oxidative MyHC-1 fiber, that confirms data on NMES-dependent atypical fiber
539 adaptation already present in literature (20). Moreover, it could be that NMES
540 protocol has to be performed with other strategies, such as active training, to reduce
541 MPC general oxidation (4). Interestingly, the increased proportion of MyHC-1 fibers

542 at post-NMES along with reduced $O_2\bullet^-$ production and no interference with the
543 oxidative status, let think that NMES could be an healthy treatment for elderly.

544 The idea that miRNAs may regulate and be regulated by oxidative stress
545 following active and/or passive exercise in skeletal muscle still awaits experimental
546 validation. However, in other cellular model such as neuron, endothelial,
547 cardiomyocytes it has been established a specific miRNA regulation by oxidant level
548 (28, 35, 59). Yildirim and coworkers (60) demonstrated a relationship between
549 increase of oxidative stress and down-regulation of miR-1, miR-133a and miR-133b
550 in rat cardiomyocytes.

551 Recently, we demonstrated human regulation of miRNAs by $O_2\bullet^-$ production
552 linked to low-intensity exercise. Indeed, we observed that human MPCs that
553 decreased $O_2\bullet^-$ production showed up-regulation of miR-1, miR-133b and miR-206,
554 while those that increased $O_2\bullet^-$ showed down-regulation of these myo-miRNAs (34,
555 48).

556 Accordingly, the decreased $O_2\bullet^-$ production up-regulated these myo-miRNAs,
557 along with miR-133a, which promoted (or supported) the myogenesis process, and
558 confirmed the positive role of the NMES protocol.

559 Nakasa and colleagues (38) demonstrated that local injection of miR-1, miR-
560 133 and miR-206 mixture in rat skeletal muscle increased muscle regeneration via
561 increased myogenic regulator factors as myogenin. Furthermore, up-regulation of
562 miR-1, miR-133a/b and miR-206 might be linked to reduction of muscle inflammation
563 (19), which would also be consistent with a reduction in the $O_2\bullet^-$ levels as a positive
564 effect of the NMES protocol. Moreover, it has been demonstrated that miR-133 and
565 miR-1 expression is linked to the regulation of apoptotic pathways (10). Although we
566 did not obtain information about this specific pathway here, we believe that the up-

567 regulation of both miR-1 and miR-133a/b could be in line with apoptosis repression,
568 in favor of cell proliferation (9, 24, 48).
569 One of the most important effects of stimulation of the skeletal muscle regeneration
570 process, which in the present case relates to MPC fusion with myofibers, is the
571 increased cross sectional area and isometric strength of myofibers, and as a direct
572 consequence, the increase in muscle strength. The isometric maximal voluntary
573 strength of lower limbs measured on post-NMES significantly increased with respect
574 to pre-NMES, accordingly with the present literature (11, 23). Interestingly, we found
575 other NMES positive effects on elderly mobility, as revealed by FTSST and TUG
576 functional tests. These effects reveal an important physiological outcome of this
577 NMES-dependent activation of skeletal muscle regeneration and suggest that NMES
578 may thus be further considered for counteract sarcopenia. Indeed, even if one
579 limitation of this method could be the discomfort that is associated with the intensity
580 of the electrically-induced muscle contractions (31, 23), in our experience, the NMES
581 has been well tolerated by elderly. Moreover, NMES could be considered as an
582 important adjuvant in clinical approach for those individuals who are unable to
583 exercise because of orthopedic problems or other complications also considering the
584 positive effect reported in literature on energy expenditure and human metabolism
585 enhancement (22, 49).
586
587

588 **CONCLUSIONS**

589 Neuromuscular electrical stimulation is an interesting protocol for the stimulation of
590 human skeletal muscle, even if this is achieved passively and in a localized manner.
591 Although NMES is extensively used in sport and human muscle rehabilitation, there

592 is little evidence of the physiological effects and few data on regeneration of human
593 sarcopenic muscle. We have demonstrated in the present study that NMES
594 stimulates specific physiological signals for MPC regeneration, which can result in
595 increased fusion of satellite cells with existing mature myofibers of the elderly through
596 increases in $[Ca^{2+}]_{cyt}$. This process appears to be driven by overexpression of
597 myogenin that is sustained by up-regulation of myo-miRNAs, which can occur due to
598 reduced $O_2\bullet^-$ production in the MPCs stimulated by this NMES protocol. In
599 conclusion, this NMES can help muscle regeneration and increase the maximal
600 isometric strength of the lower limbs in healthy elderly subjects along with their
601 mobility.
602
603 **ACKNOWLEDGMENTS**

604 The authors would like to thank all of the subjects who volunteered to participate in
605 this study for their collaboration. The authors thank Dr Christopher Berrie for English
606 editing. This study was funded by ‘G. d’Annunzio’ University grants to TP, RM and
607 SF, and the PRIN national grants 2007AWZTHH_003 to SF and 2012N8YJC3_003
608 to TP.
609
610 **CONFLICTS OF INTEREST**

611 The authors declare that they have no conflicts of interest.
612
613 **REFERENCES**

614

615 1. **Antigny F, Koenig S, Bernheim L, Frieden M.** During post-natal human
616 myogenesis, normal myotube size requires TRPC1- and TRPC4-mediated Ca^{2+}
617 entry. *J Cell Sci* 126: 2525-2533, 2013. doi: 10.1242/jcs.122911.
618 2. **Antigny F, Konig S, Bernheim L, Frieden M.** Inositol 1,4,5 trisphosphate
619 receptor 1 is a key player of human myoblast differentiation. *Cell Calcium* 56:
620 513-521, 2014. doi: 10.1016/j.ceca.2014.10.014.
621 3. **Arnaudeau S, Holzer N, König S, Bader CR, and Bernheim L.** Calcium sources
622 used by post-natal human myoblasts during initial differentiation. *J Cell Physiol*
623 208: 435-445, 2006.
624 4. **Baar K.** Using molecular biology to maximize concurrent training. *Sports Med* 44:
625 S117-125, 2014 doi: 10.1007/s40279-014-0252-0.
626 5. **Beccafico S, Puglielli C, Pietrangelo T, Bellomo R, Fanò G, and Fulle S.** Age-
627 dependent effects on functional aspects in human satellite cells. *Ann N Y Acad*
628 *Sci* 1100: 345-352, 2007.
629 6. **Bijlenga P, Liu JH, Espinos E, Haenggeli CA, Fischer-Lougheed J, Bader CR,**
630 **and Bernheim L.** T-type alpha 1H Ca^{2+} channels are involved in Ca^{2+} signaling
631 during terminal differentiation (fusion) of human myoblasts. *Proc Natl Acad Sci*
632 *USA* 97: 7627-7632, 2000. doi: 10.1073/pnas.97.13.7627.
633 7. **Bottinelli R, Canepari M, Pellegrino MA, Reggiani C.** Force-velocity properties
634 of human skeletal muscle fibers: myosin heavy chain isoform and temperature
635 dependence. *J Physiol* 495: 573-586, 1996.
636 8. **Ceafalan LC, Popescu BO, and Hinescu ME**. Cellular Players in Skeletal Muscle
637 Regeneration. *BioMed Research International* Volume 2014, Article ID 957014,
638 2014. doi.org/10.1155/2014/957014

639 9. **Crippa S, Cassano M, and Sampaolesi M**. Role of miRNAs in Muscle Stem Cell
640 Biology: Proliferation Differentiation and Death. *Current Pharmaceutical Design*
641 18: 1718-1729, 2012.
642 10. **Di Filippo ES, Mancinelli R, Pietrangelo T, La Rovere RM, Quattrocelli M,**
643 **Sampaolesi M, and Fulle S.** Myomir dysregulation and reactive oxygen species
644 in aged human satellite cells. *Biochem Biophys Res Commun* 473: 462-470,
645 2016. doi: 10.1016/j.bbrc.2016.03.030
646 11. **Filipovic A, Kleinöder H, Dörmann U, Mester J**. Electromyostimulation--a
647 systematic review of the effects of different electromyostimulation methods on
648 selected strength parameters in trained and elite athletes. *J Strength Cond Res*
649 26: 2600-2614, 2012.
650 12. **Fisher-Wellman K, and Bloomer J**. Acute exercise and oxidative stress: a 30
651 year history. *Dynamic Medicine* 8: 1, 2009. doi: 10.1186/1476-5918-8-1
652 13. **Franceschi C, and Campisi J.** Chronic inflammation (inflammaging) and its
653 potential contribution to age-associated diseases. *J Gerontol A Biol Sci Med Sci*
654 69 Suppl 1: S4-9, 2014. doi: 10.1093/gerona/glu057
655 14. **Fulle S, Mecocci P, Fanó G, Vecchiet I, Vecchini A, Racciotti D**, **Cherubini A,**
656 **Pizzigallo E, Vecchiet L, Senin U, and Beal MF**. Specific oxidative alterations
657 in vastus lateralis muscle of patients with the diagnosis of chronic fatigue
658 syndrome. *Free Radic Biol Med* 29: 1252-1259, 2000.
659 15. **Fulle S, Di Donna S, Puglielli C, Pietrangelo T, Beccafico S, Bellomo R**,
660 **Protasi F, and Fanò G.** Age-dependent imbalance of the antioxidative system in
661 human satellite cells. *Exp Gerontol* 40: 189-197, 2005.

662 16. **Fulle S, Pietrangelo T, Mancinelli R, Saggini R, and Fanò G.** Specific
663 correlations between muscle oxidative stress and chronic fatigue syndrome: a
664 working hypothesis. *J Muscle Res Cell Motil* 28: 355-362, 2007.

665 17. **Fulle S, Sancilio S, Mancinelli R, Gatta V, and Di Pietro R.** Dual role of the
666 caspase enzymes in satellite cells from aged and young subjects. *Cell Death Dis*
667 4: e955, 2013. doi: 10.1038/cddis.2013.472

668 18. **Fujiya H, Ogura Y, Ohno Y, Goto A, Nakamura A, Ohashi K, Uematsu D,**
669 **Aoki H, Musha H, and Goto K**. Microcurrent Electrical Neuromuscular
670 Stimulation Facilitates Regeneration of Injured Skeletal Muscle in Mice. *Journal*
671 *of Sports Science and Medicine* 14: 297-303, 2015.

672 19. **Georgantas RW, Streicher K, Greenberg SA, Greenlees LM, Zhu W,**
673 **Brohawn PZ, Higgs BW, Czapiga M, Morehouse CA, Amato A, Richman L,**
674 **Jallal B, Yao Y, and Ranade K.** Inhibition of myogenic microRNAs 1, 133, and
675 206 by inflammatory cytokines links inflammation and muscle degeneration in
676 adult inflammatory myopathies. *Arthritis Rheumatol* 66: 1022-1033, 2014. doi:
677 10.1002/art.38292.

678 20. **Gondin J, Brocca L, Bellinzona E, D'Antona G, Maffiuletti NA, Miotti D,**
679 **Pellegrino MA, Bottinelli R.** Neuromuscular electrical stimulation training
680 induces atypical adaptations of the human skeletal muscle phenotype: a
681 functional and proteomic analysis. *J Appl Physiol* 110: 433–450, 2011. doi:
682 10.1152/japplphysiol.00914.2010.

683

684 21. **Guo BS, Cheung KK, Yeung SS, Zhang BT, and Yeung EW.** Electrical
685 stimulation influences satellite cell proliferation and apoptosis in unloading-
686 induced muscle atrophy in mice. *PLoS ONE* 7, e30348, 2012.

687 22. **Hamada T, Hayashi T, Kimura T, Nakao K, Moritani T**. Electrical stimulation of
688 human lower extremities enhances energy consumption, carbohydrate oxidation,
689 and whole body glucose uptake. *J Appl Physiol (1985)*. 96(3):911-916, 2004.

690 23. **Herzig D, Maffiuletti NA, Eser P**. The application of neuromuscular electrical
691 stimulation training in various non-neurological patient populations: a narrative
692 review. *Physical Medicine and Rehabilitation* 7:1167-1178, 2015.

693 24. **Huang ZP, Espinoza-Lewis R, and Wang DZ.** Determination of miRNA targets
694 in skeletal muscle cells. *Methods Mol Biol* 798: 475–490, 2012.

695 25. **Kadi F, Johansson F, Johansson R, Sjöström M, and Henriksson J.** Effects
696 of one bout of endurance exercise on the expression of myogenin in human
697 quadriceps muscle. *Histochem Cell Biol* 121: 329-334, 2004.

698 26. **Kvorning T, Kadi F, Schjerling P, Andersen M, Brixen K, Suetta C, and**
699 **Madsen K.** The activity of satellite cells and myonuclei following 8 weeks of
700 strength training in young men with suppressed testosterone levels. *Acta Physiol*
701 *(Oxf)* 213: 676-687, 2015. doi: 10.1111/apha.12404.

702 27. **La Rovere RML, Quattrocelli M, Pietrangelo T, Di Filippo ES, Maccatrozzo L,**
703 **Cassano M, Mascarello F, Barthélémy I, Blot S, Sampaolesi M, and Fulle S.**
704 Myogenic potential of canine craniofacial satellite cells. *Frontiers Aging Neurosci*
705 6: 90, 2014. doi: 10.3389/fnagi.2014.00090

706 28. **Li R, Yan G, Li Q, Sun H, Hu Y, Sun J, and Xu B.** MicroRNA-145 protects
707 cardiomyocytes against hydrogen peroxide (H_2O_2)- induced apoptosis through
708 targeting the mitochondria apoptotic pathway. *PLoS One* 7(9): e44907, 2012. doi:
709 10.1371/journal.pone.0044907.

710 29. **Liu JH, König S, Michel M, Arnaudeau S, Fischer-Lougheed J, Bader CR,**
711 **and Bernheim L.** Acceleration of human myoblast fusion by depolarization:
712 graded Ca^{2+} signals involved. *Development* 130: 3437-3446, 2003.
713 30. **Lorenzon P, Bandi E, de Guarrini F, Pietrangelo T, Schäfer R, Zweyer M,**
714 **Wernig A, and Ruzzier F.** Ageing affects the differentiation potential of human
715 myoblasts. *Exp Gerontol* 39: 1545-1554, 2004.
716 31. **Maffiuletti NA**. Physiological and methodological considerations for the use of
717 neuromuscular electrical stimulation.*Eur J Appl Physiol*. 110(2):223-234, 2010.
718 doi: 10.1007/s00421-010-1502-y.
719 32. **Mancinelli R, Pietrangelo T, La Rovere R, Toniolo L, Fanò G, Reggiani C,**
720 **and Fulle S.** Cellular and molecular responses of human skeletal muscle
721 exposed to hypoxic environment. *J Biol Regul Homeost Agents* 25: 635-645,
722 2011.
723 33. **Mancinelli R, Pietrangelo T, Burnstock G, Fanò G, and Fulle S.**
724 Transcriptional profile of GTP-mediated differentiation of C2C12 skeletal muscle
725 cells. *Purinergic Signal* 8: 207–221, 2012. doi: 10.1007/s11302-011-9266-3
726 34. **Mancinelli R, DiFilippo ES, Verratti V, Fulle S, Toniolo L, Reggiani C, and**
727 **Pietrangelo T.** The regenerative potential of female skeletal muscle upon
728 hypobaric hypoxic exposure. *Front Physiol* 7: 303, 2016. doi:
729 10.3389/fphys.2016.00303
730 35. **Marin T, Gongol B, Chen Z, Woo B, Subramaniam S, Chien S, and Shyy JY.**
731 Mechanosensitive microRNAs-role in endothelial responses to shear stress and
732 redox state. *Free Radic Biol Med* 64: 61-68, 2013. doi:
733 10.1016/j.freeradbiomed.2013.05.034

734 36. **Minetto MA, Botter A, Bottinelli O, Miotti D, Bottinelli R, and D'Antona G.**
735 Variability in muscle adaptation to electrical stimulation. *Int J Sports Med* 34: 544-
736 553, 2013. doi: 10.1055/s-0032-1321799.
737 37. **Muller FL, Liu Y, and Van Remmen H.** Complex III releases superoxide to both
738 sides of inner mitochondrial membrane. *J Biol Chem* 279: 49064-49073, 2004.
739 doi:10.1074/jbc.M407715200
740 38. **Nakasa T, Ishikawa M, Shi M, Shibuya H, Adachi N, and Ochi M.** Acceleration
741 of muscle regeneration by local injection of muscle-specific microRNAs in rat
742 skeletal muscle injury model. *J Cell Mol Med* 14: 2495-2505, 2010.
743 39. **Ohno Y, Fujiya H, Goto A, Nakamura A, Nishiura Y, Sugiura T, Ohira Y,**
744 **Yoshioka T and Goto K.** Microcurrent electrical nerve stimulation facilitates
745 regrowth of mouse soleus muscle. *International Journal of Medical Sciences* 10:
746 1286-1294, 2013.
747 40**. Paoli A, Pacelli QF, Cancellara P, Toniolo L, Moro T, Canato M, Miotti D**
748 **and Reggiani C**. Myosin isoforms and contractile properties of single fibers of
749 human Latissimus Dorsi muscle**.** *Biomed Res Int.* 2013:249398, 2013 doi:
750 10.1155/2013/249398.
751 41. **Pellegrino MA, Canepari M, D'Antona G, Reggiani C, Bottinelli R**.
752 Orthologous myosin isoforms and scaling of shortening velocity with body size in
753 mouse, rat, rabbit and human muscles. *J Physiol* 546:677-689, 2003.
754 42. **Pietrangelo T, Fioretti B, Mancinelli R, Catacuzzeno L, Franciolini F, Fanò G,**
755 **and Fulle S.** Extracellular guanosine-5'-triphosphate modulates myogenesis via
756 intermediate Ca($^{2+}$)-activated K^+ currents in C2C12 mouse cells. *J Physiol* 572(Pt
757 3): 721-733, 2006.

758 43. **Pietrangelo T, D'Amelio L, Doria C, Mancinelli R, Fulle S, and Fanò G.** Tiny
759 percutaneous needle biopsy: an efficient method for studying cellular and
760 molecular aspects of skeletal muscle in humans. *Int J Mol Med* 27: 361-367,
761 2011.
762 44. **Pietrangelo T, Mariggiò MA, Lorenzon P, Fulle S, Protasi F, Rathbone M.,**
763 **Werstiuk E, and Fanò G.** Characterization of specific GTP binding sites in
764 C2C12 mouse skeletal muscle cells. *J Muscle Res Cell Motil* 23: 107-118, 2002.
765 45. **Pietrangelo T, Puglielli C, Mancinelli R, Beccafico S, Fanò G, and Fulle S.**
766 Molecular basis of the Myogenic profile of aged human skeletal muscle satellite
767 cells during differentiation. *Exp Geront* 44: 523-531, 2009.
768 46. **Pietrangelo T, Mancinelli R, Doria C, Di Tano G, Loffredo B, Fanò-Illic G and**
769 **Fulle S.** Endurance and resistance training modifies the transcriptional profile of
770 the vastus lateralis skeletal muscle in healthy elderly subjects. *Sport Sci Health*
771 7: 19–27, 2012. doi: 10.1007/s11332-012-0107-8
772 47. **Pietrangelo T, Perni S, Di Tano G, Fanò-Illic G. and Franzini-Armstrong C.** A
773 method for the ultrastructural preservation of tiny percutaneous needle biopsy
774 material from skeletal muscle. *Int. J Mol Med* 32: 965-970, 2013.
775 doi:10.3892/ijmm.2013.1454
776 48. **Pietrangelo T, Di Filippo ES, Mancinelli R, Doria C, Rotini A, Fanò-Illic G.**
777 **and Fulle S.** Low Intensity Exercise Training Improves Skeletal Muscle
778 Regeneration Potential. *Front Physiol* 6:399,
779 2015.doi:10.3389/fphys.2015.00399.
780 49. **Porcelli S, Marzorati M, Pugliese L, Adamo S, Gondin J, Bottinelli R, Grassi**
781 **B**. Lack of functional effects of neuromuscular electrical stimulation on skeletal

782 muscle oxidative metabolism in healthy humans. *J Appl Physiol*
783 *(1985)*. 113(7):1101-1109, 2012. doi: 10.1152/japplphysiol.01627.2011.
784 50. **Powers SK, Duarte J, Kavazis AN, and Talbert EE.** Reactive oxygen species
785 are signaling molecules for skeletal muscle adaptation. *Exp Physiol* 95: 1-9,
786 2010.
787 51. **Quinlan CL, Perevoshchikova IV, Hey-Mogensen M, Orr AL, and Brand MD.**
788 Sites of reactive oxygen species generation by mitochondria oxidizing different
789 substrates. *Redox Biol* 1: 304-312, 2013.
790 52. **Sciancalepore M, Coslovich T, Lorenzon P, Ziraldo G, Taccola G**.
791 Extracellular stimulation with human "noisy" electromyographic patterns
792 facilitates myotube activity. *J Muscle Res Cell Motil*, 36: 349-357, 2015. DOI
793 10.1007/s10974-015-9424-2
794 53. **Shakirzyanova A, Valeeva G, Giniatullin A, Naumenko N, Fulle S, Akulov A,**
795 **Atalay M, Nikolsky E, and Giniatullin R.** Age-dependent action of reactive
796 oxygen species on transmitter release in mammalian neuromuscular junctions.
797 *Neurobiol Aging* 38: 73-81, 2016. doi: 10.1016/j.neurobiolaging.2015.10.02
798 54. **Snijders T, Verdijk LB, Beelen M, McKay BR, Parise G, Kadi F, and van Loon**
799 **LJ.** A single bout of exercise activates skeletal muscle satellite cells during
800 subsequent overnight recovery. *Exp Physiol* 97: 762-773, 2012. doi:
801 10.1113/expphysiol.2011.063313
802 55. **Sullivan-Gunn MJ, and Lewandowski PA.** Elevated hydrogen peroxide and
803 decreased catalase and glutathione peroxidase protection are associated with
804 aging sarcopenia. *BMC Geriatr* 13: 104, 2013. doi: 10.1186/1471-2318-13-104.

805 56. **Toniolo L, Maccatrozzo L, and Patruno M**. Fiber types in canine muscles:
806 myosin isoform expression and functional characterization. *Am J Physiol*
807 292:C1915-C1926, 2007.
808 57. **Verdijk LB.** Satellite cells activation as a critical step in skeletal muscle plasticity.
809 *Exp Physiol* 99, 1449–1450, 2014. doi: 10.1113/expphysiol.2014. 081273.
810 58. **Whitney SL, Wrisley DM, Marchetti GF, Gee MA, Redfern MS, Furman JM**.
811 Clinical measurement of sit-to-stand performance in people with balance
812 disorders: validity of data for the Five-Times-Sit-to-Stand Test. *Phys Ther.*
813 85(10):1034-45, 2005
814 59. **Xu S, Zhang R, Niu J, Cui D, Xie B, Zhang B, Lu K, Yu W, Wang X, Zhang Q.**
815 Oxidative Stress Mediated-Alterations of the MicroRNA Expression Profile in
816 Mouse Hippocampal Neurons. *Int J Mol Sci* 13: 16945–16960, 2012. doi:
817 10.3390/ijms131216945
818 60. **Yildirim SS, Akman D, Catalucci D, and Turan B.** Relationship between
819 downregulation of miRNAs and increase of oxidative stress in the development of
820 diabetic cardiac dysfunction: junctin as a target protein of miR-1. *Cell Biochem*
821 *Biophys* 67: 1397-1408, 2013. doi: 10.1007/s12013-013-9672-y.
822
823
824
825
826
827
828
829

830 **Table 1:** Anthropometric characteristics, isometric maximal voluntary contraction
831 (MVC) of lower limb and functional performance measured on healthy elderly
832 subjects before (Pre-) and after (Post-) the neuromuscular electrical stimulation
833 (NMES) protocol.

	NMES		**CONTROL**	
Characteristic	**Pre**	**Post**	**Pre**	**Post**
Weight (kg)	74.2±6.9	74.5±7.0	76.8±4.2	77.5±4.0
Height (m)	1.65±0.06	1.65±0.06	1.66±0.03	1.66±0.03
BMI (kg/m^2)	27.3±2.7	27.4±2.8	27.9±2.2	28.2±2.1
Body fat (%)	26.7±5.1	25.6±5.2	24.8±3.5	24.7±3.6
MVC (N)	546±126	605±118*	499±137	488±125
FSST (s)	7.96±0.71	6.50±0.30**	7.55±0.98	7.43±1.14
TUG (s)	6.02±1.15	4.71±0.51***	5.33±0.52	5.45±0.49

834 * Significant difference for interaction time*group for NMES (n=14) *vs* Control (n=8)
835 group (F(12642.574)= 5.014; P= 0.037; np^2= 0.200; 1-β= 0.568)
836 ** Significant difference between Pre and Post for NMES group (n= 5; F(4.056,
837 1.962)= 24.811; P= 0.001; np^2= 0.674; 1-β= 0.995) and interaction time*group for
838 NMES (n=5) vs Control (n=9) group (F(2.866, 1.962)= 17.529; P= 0.001; np^2= 0.594;
839 1-β= 0.969)
840 *** Significant difference between Pre and Post for NMES group (n= 4; F(1.972,
841 1.289)= 16.823; P= 0.002; np^2= 0.605; 1-β= 0.961) and interaction time*group for
842 NMES (n=4) vs Control (n=9) group (F(2.818, 1.289)= 24.044; P= 0.001; np^2= 0.686;
843 1-β= 0.993).
844 BMI, body mass index; BF, body fat; MVC, muscle voluntary contraction; N, Newton;
845 FSST, Five Times Sit-to-Stand Test; TUG, Timed Up and Go test.
846

847 **Table 2.** Myogenicity and differentiation features of the MPCs isolated from the
848 *Vastus Lateralis* of the healthy elderly subjects before (Pre-) and after (Post-) the
849 NMES sessions.
850

Condition	Myogenicity (%desmin$^+$)	Differentiation	
		Fusion Index (%)	%Desmin$^+$ unfused
Pre-NMES	64.9 ±4.5	46.7 ±6.9	57.0 ±9.6
Post-NMES	71.1 ±5.4	50.7 ±6.2	50.7 ±8.6

851
852
853
854 **Figure legends**
855
856 **Figure 1**. **Population doubling level of MPCs.**
857 Population doubling levels of MPCs (undifferentiated cells) obtained from the skeletal
858 muscle of six representative of the healthy elderly subjects, with respect to the days
859 of *in-vitro* cultivation of these cells, as pre-NMES (a) and post-NMES (b).
860
861 **Figure 2. Myonuclei fused with single mature myofibers.**
862 The graph shows the numbers of myonuclei for the single dissected myofibers from
863 the muscle needle biopsy of elderly subjects were counted (per 10^6 μm^3 myofiber
864 volume). The myofibers analyzed were 27 and 33 for pre- and post-NMES samples,
865 respectively. The images show an example of human fibers stained for determination
866 of myonuclear density: the nuclei are revealed with DAPI; an antibody against alpha-
867 actinin allows to determine the volume. Top, image of pre-NMES myofiber; bottom,
868 image of post-NMES myofiber. Scale bar, 20 µm.

869

870 **Figure 3. MyHC isoform distribution in biopsy samples collected before and
871 after NMES.** The MyHC isoform distribution was determined by electrophoretic
872 separation and densitometric analysis of proteins of biopsy samples from the *Vastus*
873 *Lateralis* muscle. The dark columns represent the percentages of the MyHC isoform
874 distribution on post-NMES, and the white columns represent pre-NMES percentages.
875 *$p \leq 0.05$.

876

877 **Figure 4. Phenotype and isometric tension of single fiber**
878 Single-fiber analysis, cross sectional area (A), force (B) and specific isometric tension
879 (C). The white and dark columns represent pre-NMES and post-NMES samples,
880 respectively. Panel A shows the cross-sectional area (CSA) of single muscle fibers
881 obtained by the *Vastus Lateralis*. Panel B shows the force developed by single fiber.
882 Panel C reported measurements of specific isometric tension (force/CSA) developed
883 in maximal calcium activated contraction by the same fibers. *$p \leq 0.05$

884

885 **Figure 5. Free intracellular Ca^{2+} concentrations of MPCs.**
886 (a) Free cytoplasmic Ca^{2+} concentrations of the undifferentiated MPCs as pre-NMES
887 to post-NMES, as the basal $[Ca^{2+}]_{cyt}$ (*, $p < 0.05$) and (b) the time-course of the
888 thapsigargin-dependent Ca^{2+} release. (c) Area under the curve measures for the
889 $[Ca^{2+}]_{cyt}$ of the undifferentiated MPCs, as pre-NMES to post-NMES, for estimation of
890 the thapsigargin-sensitive Ca^{2+} stores released over the first 2 min of thapsigargin
891 stimulation (***, $p < 0.0001$).

892

Figure 6. Gene expression of early transcriptional and myogenic regulatory factors.

Pre-NMES to post-NMES mRNA expression levels (as ΔCt) for *Pax3*, *Pax7*, *Myf5*, *MyoD*, and *myogenin* gene expression. Data are means ± SE from three independent experiments, each performed in triplicate. (*, $p <0.05$ and ***, $p <0.0001$)

Figure 7. Superoxide anion production and superoxide enzymatic dismutation.

Quantitative analyses from pre-NMES to post-NMES in MPCs for $O_2^{\bullet -}$ (a) and the activity of the enzyme superoxide dismutase, SOD (b). The SOD units (U_{SOD}) were calculated considering that 1 SOD unit is defined as the quantity that inhibits the rate of cytochrome c reduction by 50% per ng of protein (b). ***, $p <0.0001$

Figure 8. SOD1 and SOD2 protein expression.

Western blotting analysis of superoxide enzymes cytosolic type 1, and mitochondrial type 2. The panel a shows representative bands of SOD1 and SOD2 enzymes obtained by MPCs from *Vastus Lateralis* muscles biopsies before (pre-) and after (post-) NMES. Panel b and c show the SOD2 and SOD1 protein quantification.

*, $p <0.05$, n=4

Figure 9. **miRNA expression**.

Pre-NMES to post-NMES relative expression (as ΔCt) of miR-133a, miR-133b, miRNA-1, and miR-206 (as indicated) in MPCs. Data are means ± SE from three independent experiments, each performed in triplicate. ***, $p <0.0001$

a

PRE-NMES

pdl

20
15
10
5
0

0
50
100

Time (days)

b

POST-NMES

pdl

20
15
10
5
0

0
25
50
75
100

Time (days)

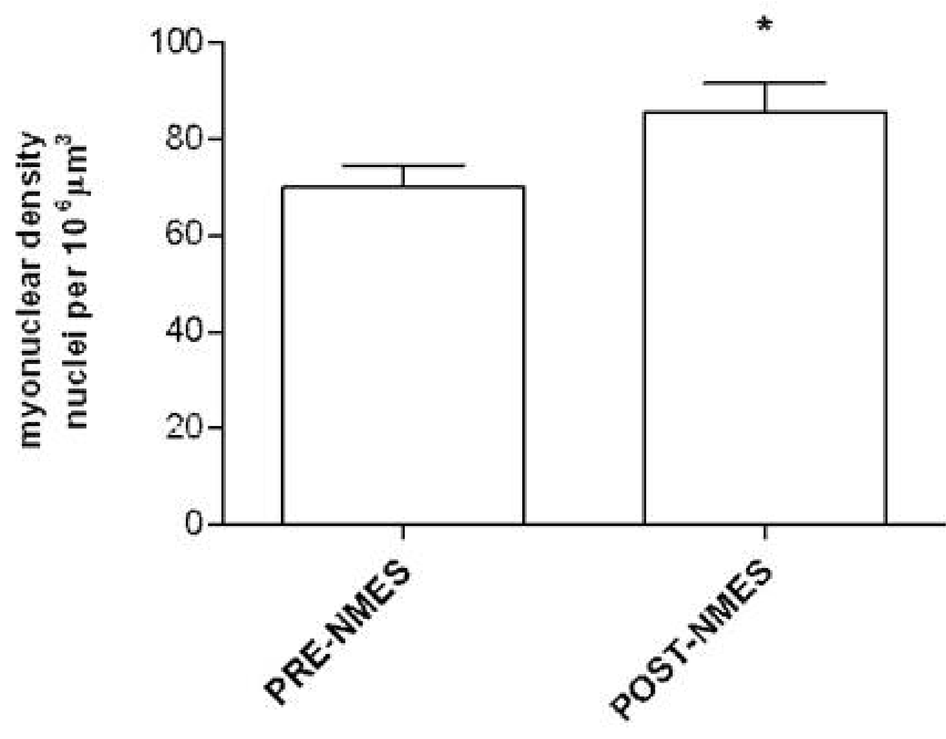

*
100
80
60
40
20
0
myonuclear density
nuclei per $10^6 \mu m^3$
PRE-NMES
POST-NMES

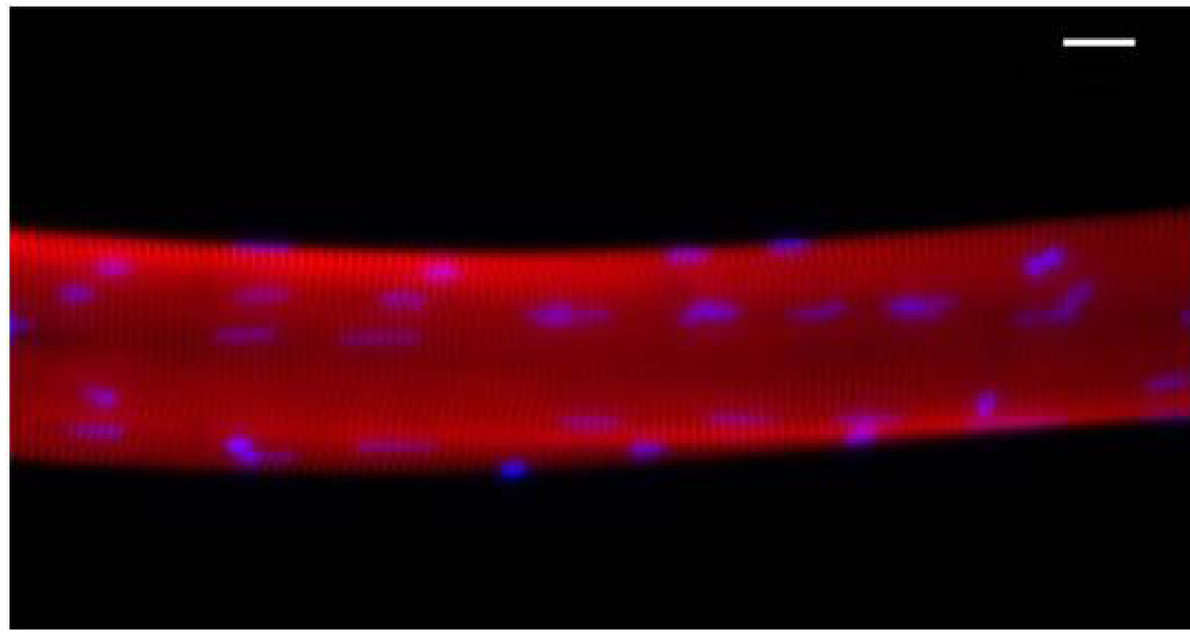

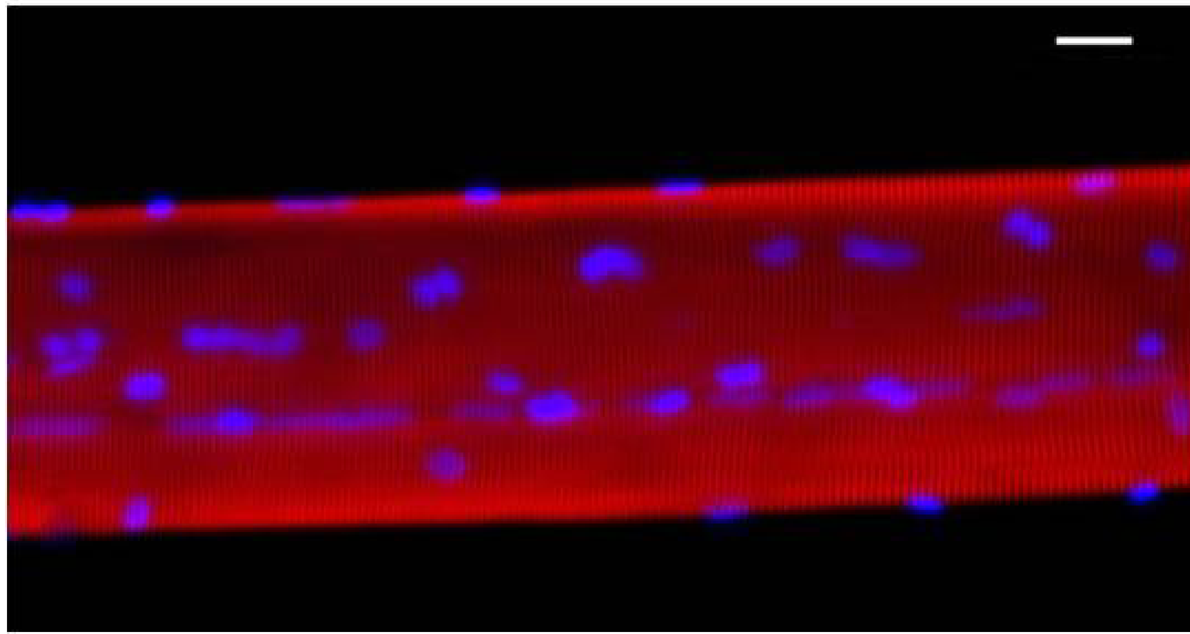

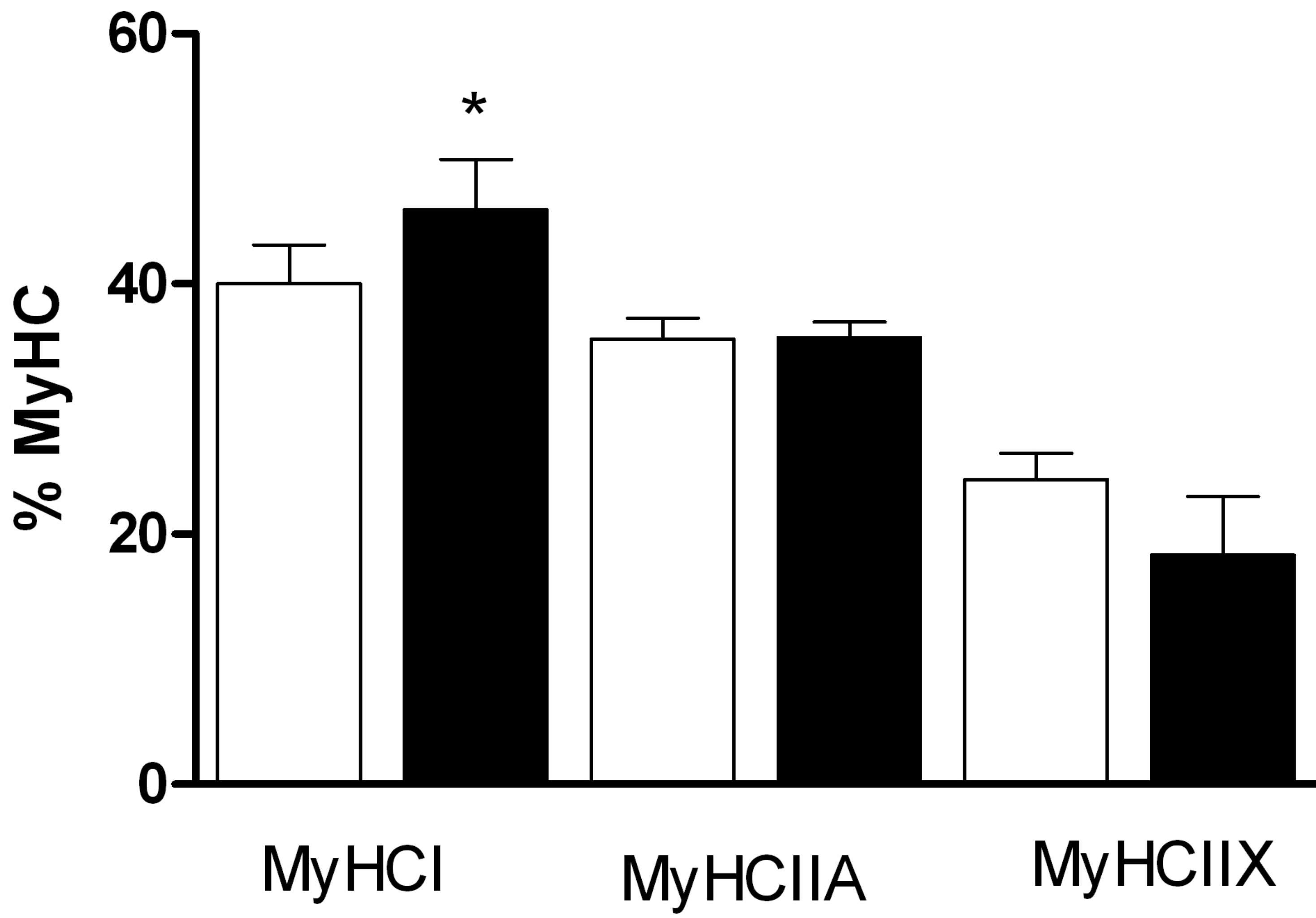
60
40
20
0
% MyHC
*
MyHCI
MyHCIIA
MyHCIIX

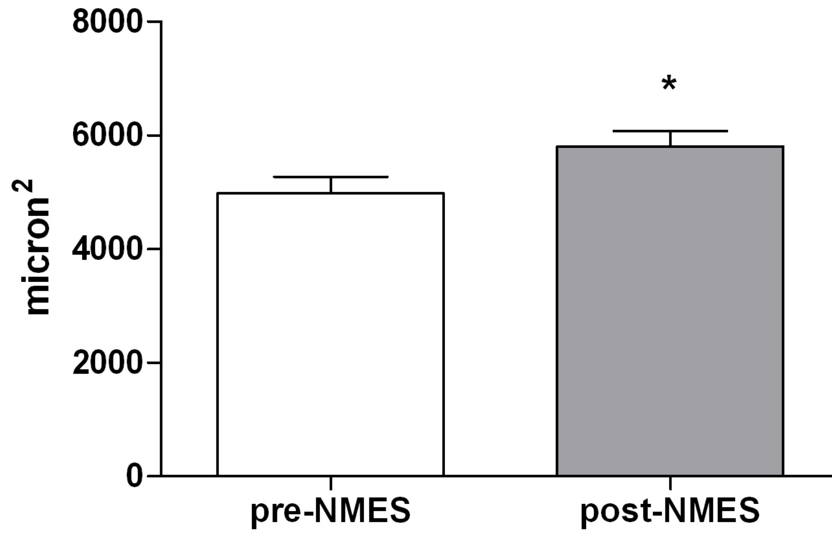
CSA
8000
6000
4000
2000
0
micron^2
*
pre-NMES
post-NMES

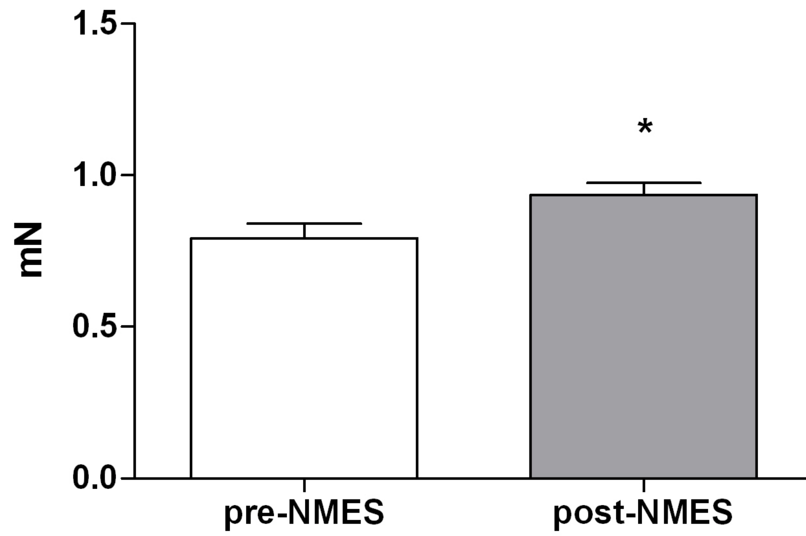
Force
1.5
1.0
0.5
0.0
mN
*
pre-NMES
post-NMES

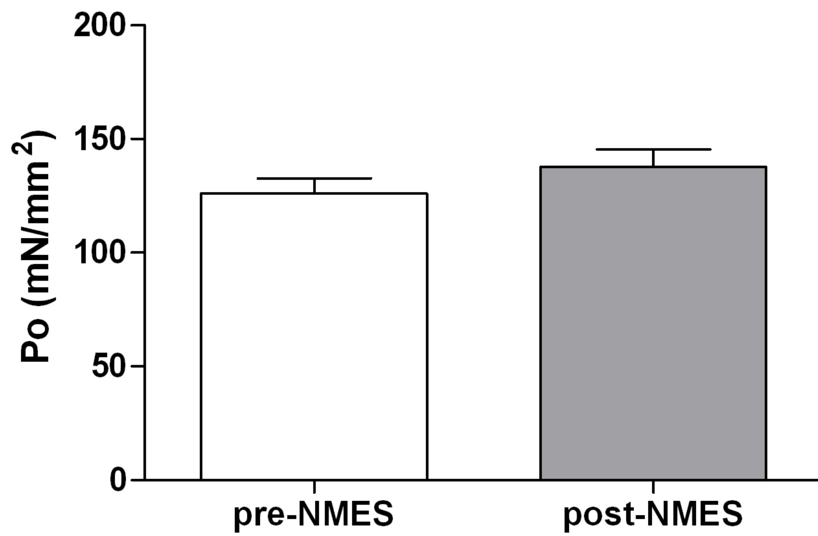
Tension
200
150
100
50
0
Po (mN/mm^2)
pre-NMES
post-NMES

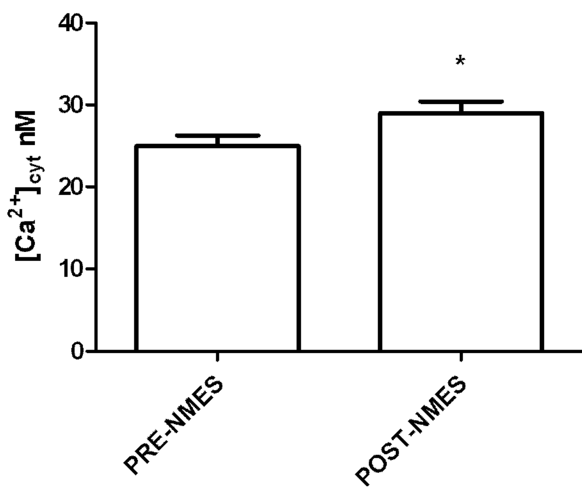
a
40
30
20
10
0
[Ca2+]cyt nM
*
PRE-NMES
POST-NMES

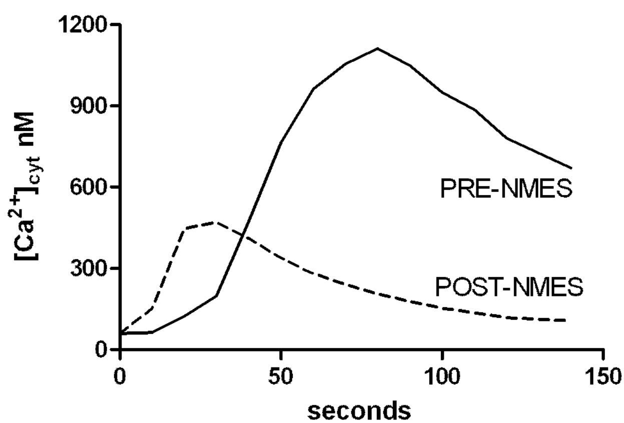
b
1200
900
600
300
0
[Ca2+]cyt nM
PRE-NMES
POST-NMES
0
50
100
150
seconds

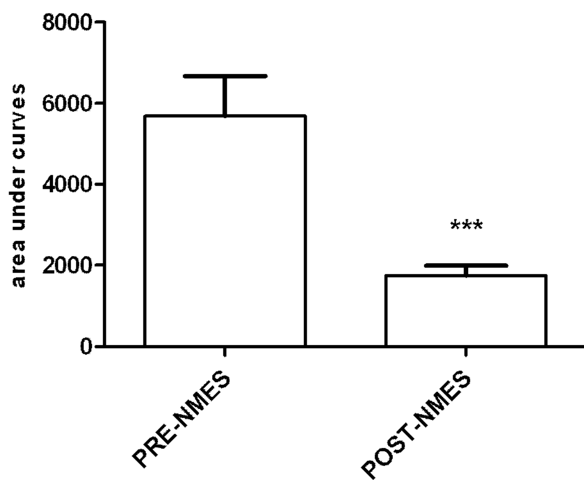
c
8000
6000
4000
2000
0
area under curves
***
PRE-NMES
POST-NMES

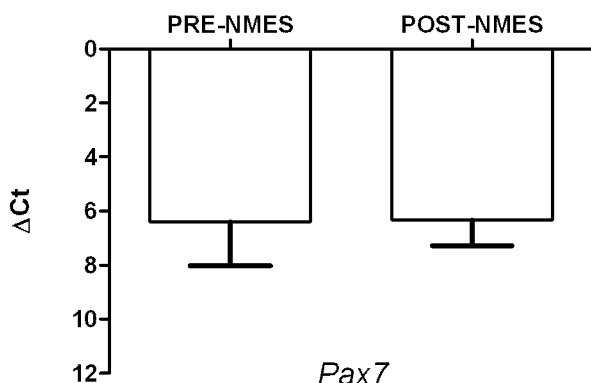
Pax3
PRE-NMES
POST-NMES
ΔCt
0
2
4
6
8
10
12

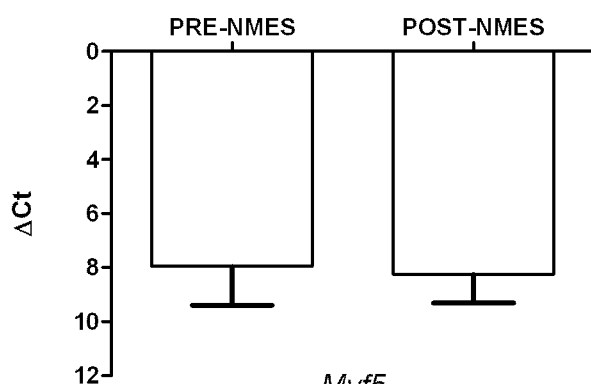
Pax7
PRE-NMES
POST-NMES
ΔCt
0
2
4
6
8
10
12

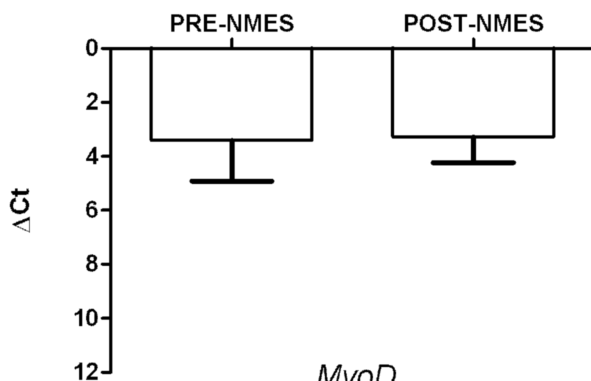
Myf5
PRE-NMES
POST-NMES
ΔCt
0
2
4
6
8
10
12

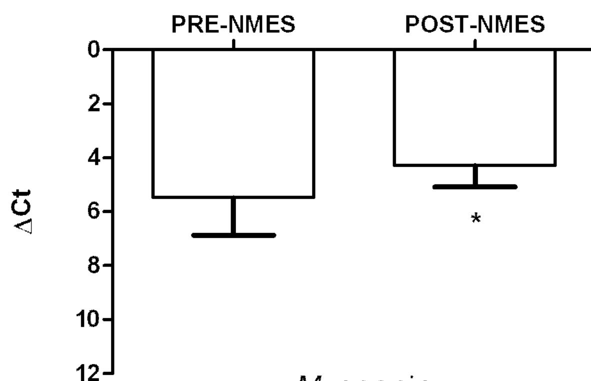
MyoD
PRE-NMES
POST-NMES
ΔCt
0
2
4
6
8
10
12
*

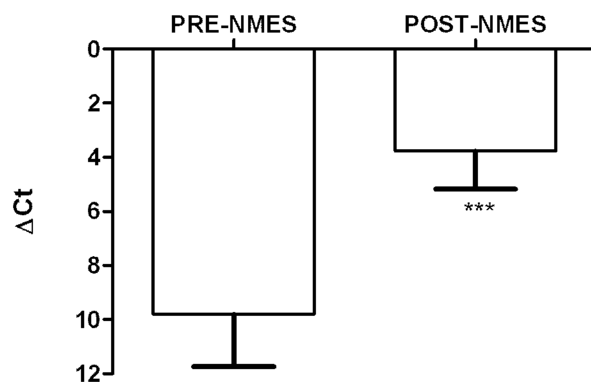
Myogenin
PRE-NMES
POST-NMES
ΔCt
0
2
4
6
8
10
12
***

a

$O_2^{\cdot -}$ reduction

0.25
0.20
0.15
0.10
0.05
0.00

O.D. $_{550nm}$/ 1×10^6 cells

***

PRE-NMES
POST-NMES

b

SOD activity

40
30
20
10
0

U_{SOD} ng^{-1}

PRE-NMES
POST-NMES

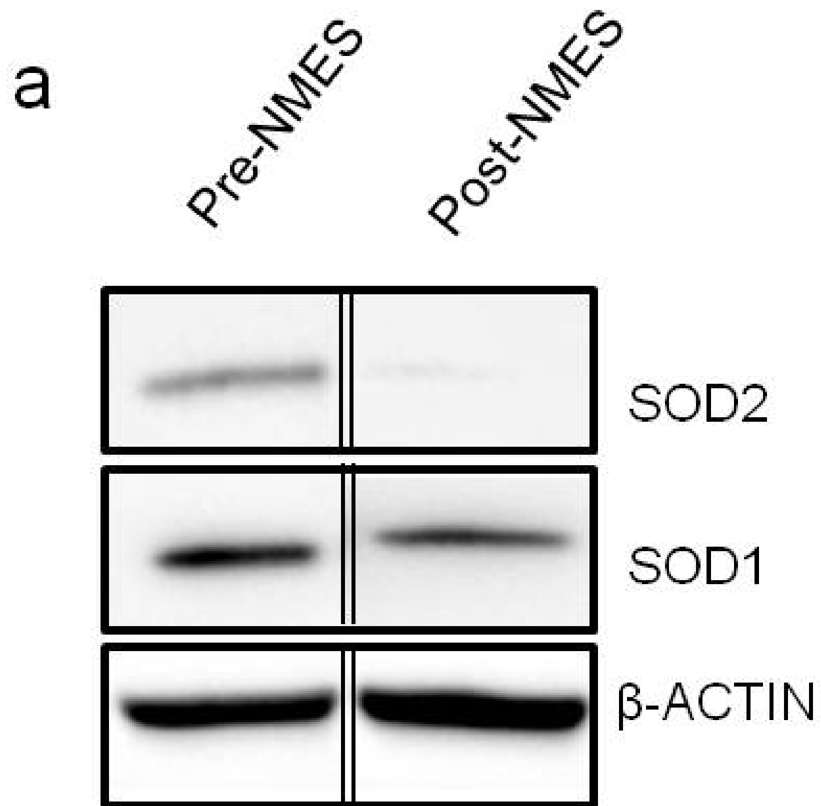
a
Pre-NMES
Post-NMES
SOD2
SOD1
β-ACTIN

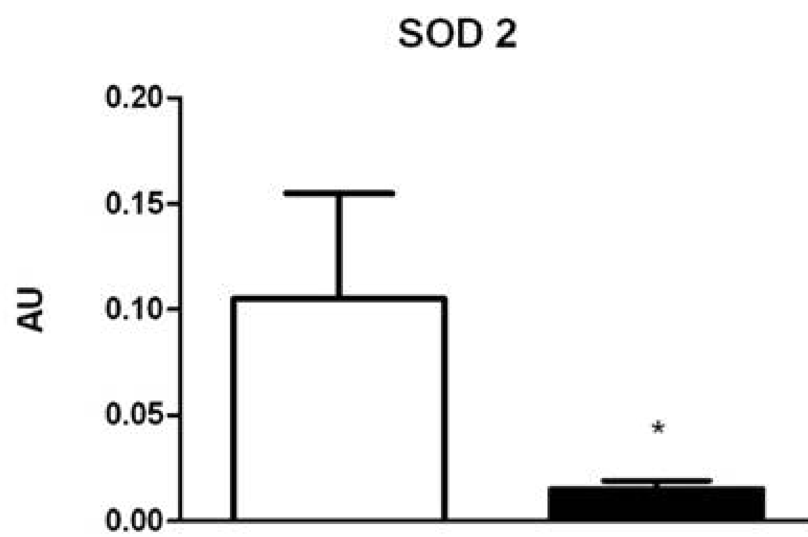
SOD 2
0.20
0.15
0.10
0.05
0.00
AU
*

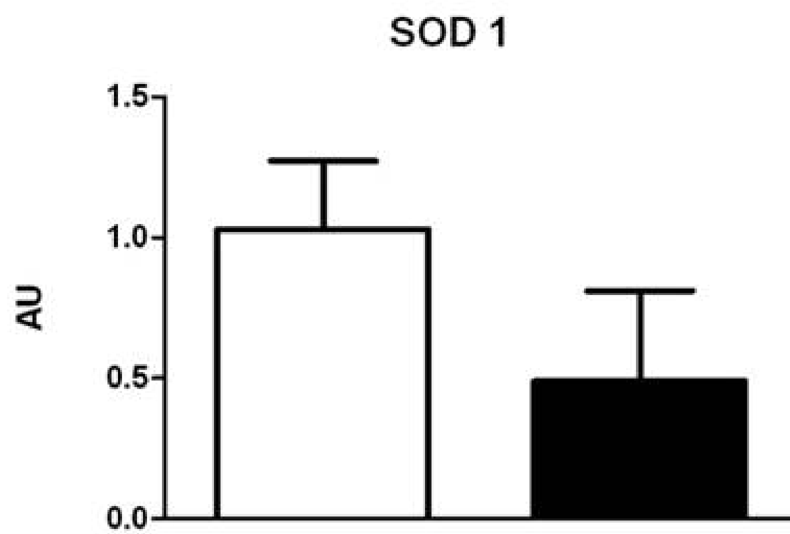
SOD 1
1.5
1.0
0.5
0.0
AU

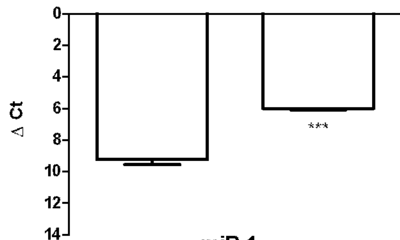
miR-133a
Δ Ct
0
2
4
6
8
10
12
14
***

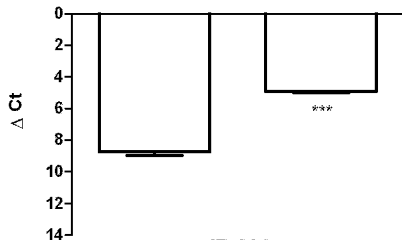
miR-133b
Δ Ct
0
2
4
6
8
10
12
14
***

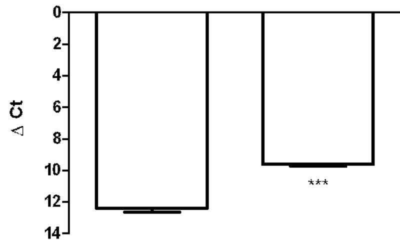
miR-1
Δ Ct
0
2
4
6
8
10
12
14
***

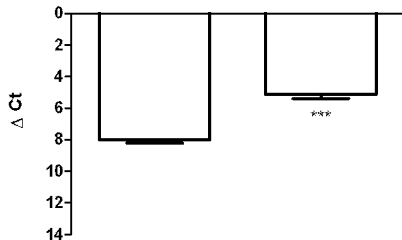
miR-206
Δ Ct
0
2
4
6
8
10
12
14
***